

In situ surface-enhanced Raman spectroscopy study of thiocyanate ions adsorbed on silver nanoparticles under high pressure

Pan Wang^{a,b}, Heping Li^{a,*}, Can Cui^a, Jianjun Jiang^a

^a Key Laboratory of High-temperature and High-pressure Study of the Earth's Interior, Institute of Geochemistry, Chinese Academy of Sciences, Guiyang 550081, China

^b University of Chinese Academy of Sciences, Beijing 100049, China

ARTICLE INFO

Keywords:

High pressure
Thiocyanate ion
In situ SERS
Diamond-anvil cell

ABSTRACT

The pressure-dependent C-N stretching mode, ν_{C-N} , for thiocyanate ions adsorbed at the silver nanoparticles-aqueous interface is examined in situ by surface-enhanced Raman spectroscopy (SERS) via a commonly used diamond anvil cell in the experimental pressures range from 31 MPa to 943 MPa. The spectroscopic measurements show that three different geometries are adopted by thiocyanate ions adsorption simultaneously at high pressure. The stretching mode ν_{C-N} of S-bound around 2120 cm^{-1} exists throughout the whole pressure range and the intensity of ν_{C-N} of N-bound around 2070 cm^{-1} increased with the pressure. The ν_{C-N} of bridge-bound coexist with the stretching mode ν_{C-N} of S-bound and N-bound in the form of weak peaks around 2220 cm^{-1} at the pressures range from 627 MPa to 943 MPa. Current results demonstrate that high pressure promotes the N-bound and bridge-bound adsorption of thiocyanate ions on the surface of silver nanoparticles.

1. Introduction

Owing to its high molecular specificity and high sensitivity, surface-enhanced Raman scattering (SERS) has been developed to be a very promising approach in detecting trace amounts of molecules in the past few decades [1–4]. Unfortunately, SERS did not developed to be a commonly used surface analysis technology as many people had expected because of some obstacles. One of the obstacles is that there is no clear mechanism to explain all of the observed phenomena. There has been the consensus that a chemical enhancement and an electromagnetic enhancement contributing to the major SERS effect [5]. To explain all SERS phenomena quantitatively, in situ high pressure technology are required due to the different molecular information under high pressure.

To date, there have been a few previous studies involving Raman scattering of adsorbed molecules under high pressures. Podini and Schnur firstly observed the Raman spectrum of pyridine adsorbed to silver island film under high pressure in a Keyes pressure cell [6]. According to their experiment, an irreversible loss in the Raman intensity was observed when pressure increased. Sandroff and his co-workers carried out a detailed experiment of three molecules on gold and silver colloids in a diamond anvil cell up to 26 kbar [7]. The frequency shifts and changes in the line widths as a function of the pressure were focused by the above researchers, which were different from the SERS

phenomenon at ambient pressure. Efrima et al. demonstrated some initial work with metal liquid-like films (MELLFs) and colloids under high pressure [8]. They found the pressure-induced large blue shifts of the vibrational frequencies adsorbed species and vibrational modes which were screened from the effect of the external pressure by the rigid and nonisotropic nature of the adsorbed layer. Dlott's group gave a series of excellent studies of molecular monolayers in a DAC combined with SERS technology [9–12]. In our previous work, we have conducted the in situ SERS detection in high pressure solution by using a DAC, where the 4-chlorothiophenol solution with a concentration of $1 \times 10^{-10}\text{ mol/L}$ was detected at 978 MPa [13]. Because of the different SERS information at high pressures mentioned above, more explorations with specific molecules should be carried in high pressure SERS studies.

The thiocyanate ion (SCN^-) has been commonly used as a target analyte in spectroscopy studies due to its well-known structure. According to Geerlings et al. [14] and Li et al. [15], free SCN^- exhibits two canonical forms, as shown in Eq. (1):



Because of the special form, three adsorption ways will happen when SCN^- is attached to a metal surface and the orientation of adsorbed SCN^- can be S-bound, N-bound, or bridge bound [16,17]. Obviously, the frequency of C-N stretching mode is sensitive to the adsorption geometry of SCN^- and depends on the potential of the metal

* Corresponding author at: No. 99, Lincheng West Road, Guanshanhu District, Guiyang 550081, China.

E-mail address: liheping@vip.gyig.ac.cn (H. Li).

<https://doi.org/10.1016/j.chemphys.2018.08.029>

Received 10 May 2018; Accepted 15 August 2018

Available online 17 August 2018

0301-0104/ © 2018 Elsevier B.V. All rights reserved.

(via the Stark effect) [17]. Because of these features of SCN^- , a great deal of SERS studies has been conducted using SCN^- as model analyte, especially in electrochemical SERS studies [14,18–23]. Potential-dependent SCN^- adsorption on electrodes were conducted and they came to conclusions that the *N*-bound SCN^- adsorption occurred at the lower potential region, the middle potential region benefited from *S*-bound SCN^- adsorption, and the bridging geometry was deemed to be found at the higher potential region. In most cases, there is only one adsorption mode in normal SERS experiments without potential changes [24,25].

Considering the different phenomenon to occur under high pressures, we present a study on the SERS of SCN^- adsorbed at silver nanoparticles (Ag NPs) under high pressure by using a diamond-anvil cell. The pressure-dependent behavior of SCN^- adsorbed at Ag NPs was studied in a wide pressure range. The *S*-bound SCN^- was observed during the whole pressure range and the intensity of the *N*-bound increases gradually with the increase of pressure. The bridge bound was found with a weak peak when the pressure increased to a very high value. In the high-pressure region, these three kinds of adsorption occurred simultaneously, which is not visible in conventional SERS studies and even in electrochemical SERS studies.

2. Experimental section

2.1. Chemicals

Sodium thiocyanate, the target analyte in our experiment, was obtained from Aladdin Industrial Corporation (Shanghai, China). The poly (allylamine hydrochloride) (PAH), having an average molecular weight of 900,000 Da, were purchased from Sigma-Aldrich Company. Silver nitrate, trisodium citrate dehydrate, and sodium chloride were purchased from Sinopharm Chemical Reagent Corporation (Shanghai, China). All chemicals in the experiments were analytic reagents and were prepared with ultrapure water.

2.2. Experimental

The Ag NPs were prepared by the classical chemical reduction method [26]. After centrifugation and diluted with ultrapure water, the Ag NPs suspension was characterized by a JEM-2000FXII transmission electron microscope. The ultraviolet absorption spectrum of the suspension was conducted on a Cary 5000 spectrophotometer. Oćwieja's method [27] was used to assemble the Ag NPs on the silicon wafer and the preparation of the SERS substrate was described in detail in our previous paper [13]. Fig. 1 shows the schematic of the diamond anvil cell (DAC) apparatus with quartz pressure sensors and self-assembled substrate for SERS from 1×10^{-5} mol/L sodium thiocyanate solution.

The high-pressure SERS experiments were performed in a Renishaw in-Via confocal micro-Raman spectrometer, with excitation at 514.5 nm. The laser was focused with a $20 \times$ objective and the laser power was set to 80 mW. To avoid CCD saturation and reduce the noise, 3 spectra were accumulated for each acquisition and the integration time for each spectrum was 20 s.

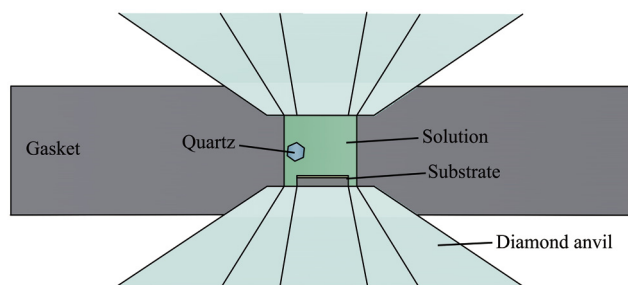


Fig. 1. The sample loading of the SERS experiments in DAC.

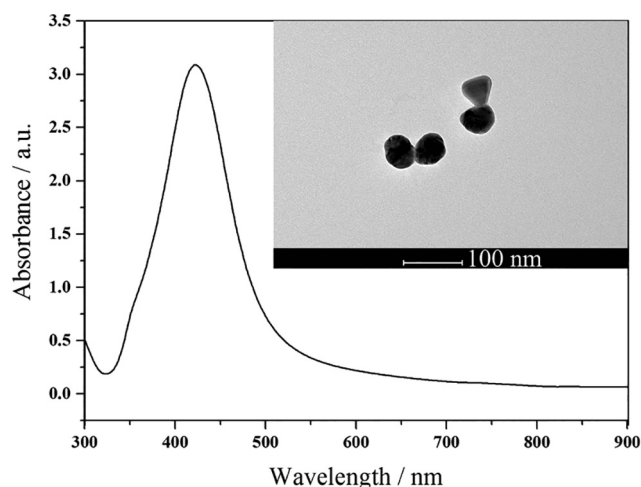


Fig. 2. The absorption spectrum of the Ag NPs suspension. The inset is the transmission electron micrograph of Ag NPs.

3. Results and discussion

To characterize the absorption properties of the obtained Ag NPs, the UV–vis spectrophotometer was used. The suspension showed an intensive visible absorption band near 422 nm, attributed to the surface plasmon absorption of Ag NPs [28], see Fig. 2. The narrow and symmetric plasmon band indicates that there were few agglomerated particles in the suspension [27,29,30]. The TEM characterization (Fig. 2 inset) also implied that the particles were well-dispersed and the diameter of the particles was about 50 nm. The size of the Ag NPs enabled the substrate to obtain high sensitivity for SERS experiments. It is necessary for the SERS substrate to have a high sensitivity because SERS intensity drops dramatically when samples are loaded in the DAC [12,13]. On the one hand, high pressure can destroy a number of Ag NPs, which decreased the number of SERS-active “hot spot”. On the other hand, the pressure-driven deformation of NPs caused the absorption spectra broad and red shift [31], which is negative to the intensity of SERS.

The pressures in the DAC were determined by spectroscopy method proposed by Schmidt et al. [32], and the accuracy of the pressure determination was ± 50 MPa. The Raman spectra of quartz at different pressures and the calculated pressures are shown in Fig. 3. The pressure at 31 MPa was measured at once when the chamber was sealed. As the experiment going on, the other pressures were measured step by step.

We measured the Raman spectra of SCN^- adsorbed on Ag NPs in situ inside the DAC at various pressures ranging from 31 MPa to 943 MPa, as shown in Fig. 4. The Raman peaks showed in the figure are

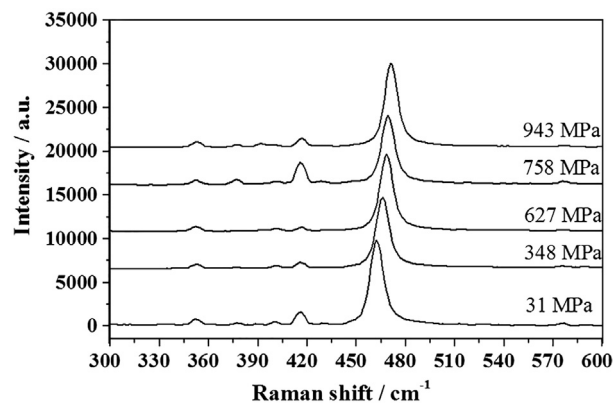


Fig. 3. Raman scattering showing the ν_{464} cm^{-1} of quartz in the DAC at different pressures.

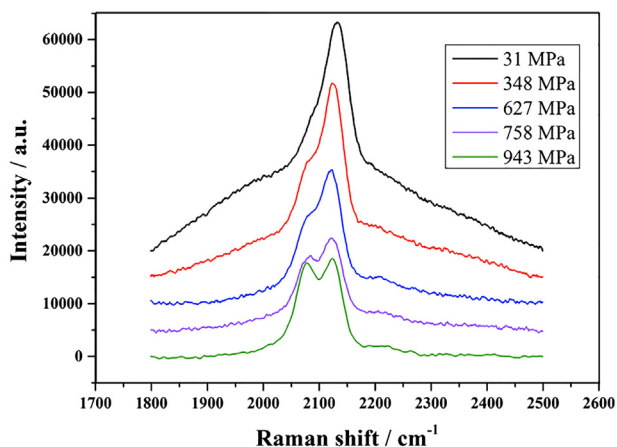


Fig. 4. SERS spectra of SCN^- from self-assembled Ag NPs under various pressures ranging from 31 MPa to 943 MPa at room temperature.

the C-N stretching mode [16,33]. It is important to note that an obvious new Raman peak appeared around 2070 cm^{-1} at 348 MPa and existed in the follow-up pressures. According to Gans et al. the peak near 2070 cm^{-1} corresponds to the $\nu_{\text{C-N}}$ of *N*-bound [34]. In addition, we found a peak with low intensity around 2220 cm^{-1} when the pressure in the chamber of DAC reached to 627 MPa. The peak around 2220 cm^{-1} corresponds to the $\nu_{\text{C-N}}$ of bridge-bound [32]. It should be noted that a band around 2120 cm^{-1} appears throughout the whole pressure region, which is well-known to be the stretching mode $\nu_{\text{C-N}}$ of S-bound SCN^- [16,18,19,35].

In order to see the changes of $\nu_{\text{C-N}}$ more clearly as the pressure increases, we plot the spectra at different pressure ranges on two figures, as shown in Fig. 5. It is obvious that a peak with low intensity around 2220 cm^{-1} appeared at 627 MPa, which is marked in rectangular box in Fig. 5(a). We have already known that it is the stretching mode $\nu_{\text{C-N}}$ of bridge-bound. In addition, a shoulder peak around 2070 cm^{-1} corresponds to the stretching mode $\nu_{\text{C-N}}$ of *N*-bound appeared in this pressure range. The SERS spectra in Fig. 5(b) correspond to pressures of 627 MPa, 758 MPa, and 943 MPa, respectively. The stretching mode $\nu_{\text{C-N}}$ of bridge-bound existed through this pressure range and the intensity of the peak has no obvious change. Instead, a marked increase has taken place for the stretching mode $\nu_{\text{C-N}}$ of *N*-bound and the peak intensity at 943 MPa exceeded the intensity at 758 MPa, as shown in rectangular box in Fig. 5(b). This may be a dynamic progress. The increased pressure promoted the adsorption of *N*-bound SCN^- and the bridge one. Three possible situations will be happened in this progress. Firstly, free SCN^- in the chamber adsorbed in these three forms with the pressure increased. Secondly, bridge adsorption turned to S site or N site

adsorption. Finally, the other sites of S-bound or *N*-bound were forced to continue to adsorb, which formed the bridge-bound adsorption. It should be sure that these three kinds of adsorption interconvert and different sites continuously desorbing and adsorbing on the surface of Ag NPs.

What should be concerned in this experiment is that the pressure-transmitting medium we used is aqueous thiocyanate solution. 943 MPa is quite closed to the phase transition point of water. In Fig. 5(b), the bridge-bound adsorption appeared at 627 MPa, we suggested that low density water converted to high density water and ice appears in the chamber during the pressurization. In part the change of water at high pressure affect the adsorption of SCN^- .

These three kinds of adsorption could not occur simultaneously at the same potential even in the electrochemical SERS studies. This is an interesting and intriguing discovery of this experiment, which suggests that the study of SERS in situ under high pressure will play a certain role in the study of SERS mechanism.

We have discussed the reasons for the SCN^- adsorbed on the surface of Ag NPs in three ways under high pressures. To further understand the effects of pressure on the adsorption of SCN^- on the surface of Ag NPs, we gradually reduced the pressure in the DAC to 45 MPa after the chamber pressure reached to 943 MPa. Compared with the SERS spectra at 45 MPa and 31 MPa, we find that the stretching mode $\nu_{\text{C-N}}$ of *N*-bound still exists as a shoulder peak and the stretching mode $\nu_{\text{C-N}}$ of bridge-bound has completely disappeared, as shown in Fig. 6. This strongly suggested that the *N*-bound adsorption and bridge adsorption were forced to occur on the surface of Ag NPs under high pressure without potential applied. As shown in Fig. 6, the chamber volume of the DAC at 943 MPa is much smaller than the volume at 31 MPa. The increased pressure increases the SCN^- number density and also changes the binding energy differently for each site. The appearance of the new species, the bridge site, seems to occur because the binding energy of the bridge site is lowered more than other sites. It seems that the increased pressure make the *N*-bound adsorption more stable and the bridge-bound occurred, which make these two adsorption forms easier detected by Raman spectroscopy because the more stable forms would be more polar with the higher absorption cross section. There is only one kind of $\nu_{\text{C-N}}$ for SCN^- adsorbed at the Ag NPs without potential even the concentration at a very high value. This phenomenon indicates that density effect makes the *N*-bound and bridge-bound easier to occur and the electronic one plays a key role in this progress. With the decreased of the pressure in the chamber, the binding energy of *N*-bound and bridge-bound returned to normal value, which caused the number of SCN^- adsorbed by the *N*-bound and bridge-bound drastically reduced and the stretching mode $\nu_{\text{C-N}}$ of bridge-bound could not be reflected in the SERS spectrum. As the pressure decreased to 45 MPa, the intensity of the stretching mode $\nu_{\text{C-N}}$ of S-bound was stronger than that

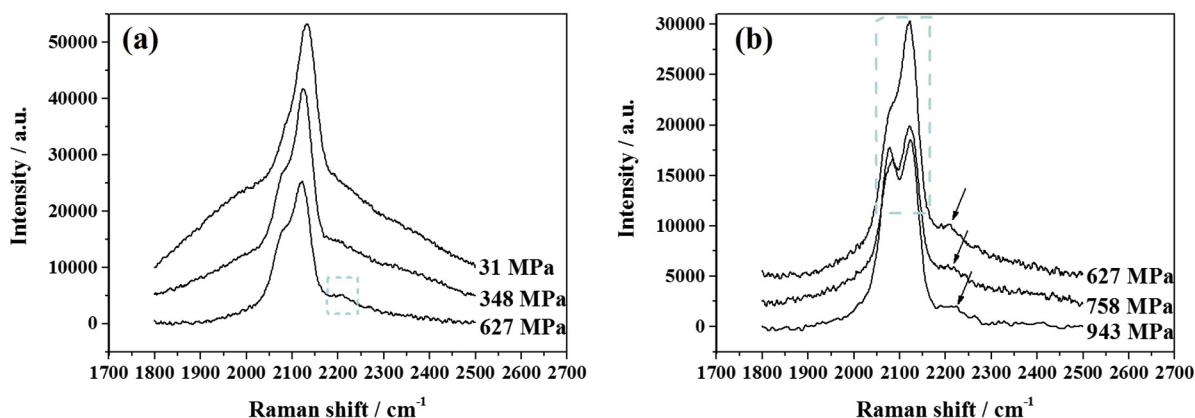


Fig. 5. (a) SERS spectra of SCN^- from self-assembled Ag NPs at 31 MPa, 348 MPa, 627 MPa, respectively; (b) SERS spectra of SCN^- from self-assembled Ag NPs at 627 MPa, 758 MPa, 943 MPa.

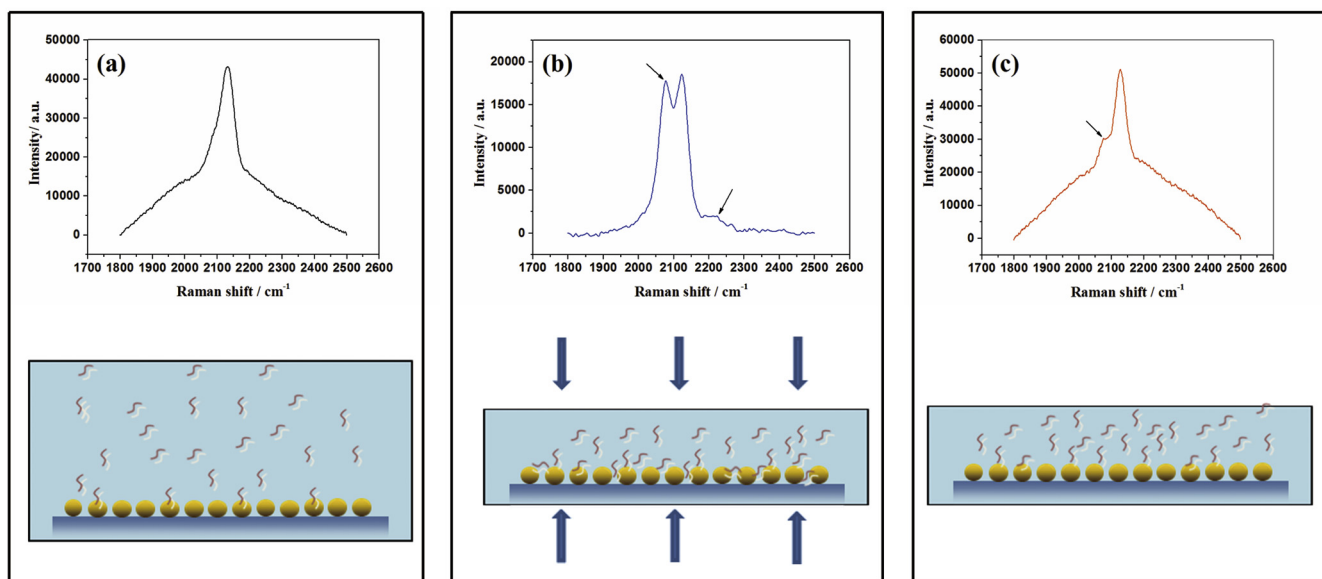


Fig. 6. (a) Is the SERS spectra of SCN^- from Ag NPs at 31 MPa. (b) Is the SERS spectra of SCN^- from Ag NPs at 943 MPa and (c) is the SERS spectra of SCN^- from Ag NPs at 45 MPa (reduced from 943 MPa).

at 31 MPa, which suggests that the pressurization process caused more SCN^- adsorbed on the surface of Ag NPs via S-bound and the activity of the SERS substrate can be basically restored to the state at 31 MPa.

4. Conclusion

In this study, we have obtained the in situ SERS of sodium thiocyanate solution at high pressure and ambient temperature conditions in DAC. S-bound adsorption, N-bound adsorption and bridge-bound were found under high pressure simultaneously for the first time. The current results suggest that S-bound adsorption existed throughout the experimental pressure range. As the pressure increased, the intensity of the stretching mode $\nu_{\text{C-N}}$ of N-bound became stronger. When the pressure reached to 627 MPa, the stretching mode $\nu_{\text{C-N}}$ of bridge-bound appeared and coexisted with the stretching mode $\nu_{\text{C-N}}$ of N-bound and S-bound. The intensity of the stretching mode $\nu_{\text{C-N}}$ of bridge-bound has no obvious change as the pressure increased to 943 MPa, but the intensity of the stretching mode $\nu_{\text{C-N}}$ of N-bound become stronger. When the pressure was relieved to 45 MPa, the bridge-bound adsorption disappeared and the intensity of N-bound adsorption peak reduced and S-bound adsorption peak become stronger, which suggest that the appearance of N-bound adsorption and bridge-bound adsorption were forced by high pressure and the activity of the SERS substrate can be basically restored from high pressure. The obtained results in our work demonstrate the merits of high pressure SERS in studying molecule adsorption at metal interfaces and high-pressure SERS can be used as an effective method to study the mechanism of SERS in the future.

Acknowledgements

The authors would like to thank Shirong Liu for his technical support with the TEM measurements and Wei Mao for his great deal of useful advice at State Key Laboratory of Ore Deposit Geochemistry, Institute of Geochemistry, Chinese Academy of Sciences (CAS). We also would like to thank Rui Li and Bing Mo for their experimental support with the UV-vis adsorption spectra at the Center for Lunar and Planetary Sciences, Institute of Geochemistry, Chinese Academy of Sciences (CAS). This research is supported by the National Key Research and Development Plan of China (2016YFC0600104) and the “135” Program of the Institute of Geochemistry, Chinese Academy of Sciences (CAS).

References

- [1] S.K. Islam, Y.P. Cheng, R.L. Birke, O. Green, T. Kubic, J.R. Lombardi, Rapid and sensitive detection of synthetic cannabinoids AMB-FUBINACA and α -PVP using surface enhanced Raman scattering (SERS), *Chem. Phys.* 506 (2018) 31–35.
- [2] J.A. Huang, Y.L. Zhang, Y. Zhao, X.L. Zhang, M.-L. Sun, W. Zhang, Superhydrophobic SERS chip based on a Ag coated natural taro-leaf, *Nanoscale* 8 (2016) 11487–11493.
- [3] S.C. Pinzaru, D.A. Magdas, Ag nanoparticles meet wines: SERS for wine analysis, *Food Anal. Methods* 11 (2018) 892–900.
- [4] Y. Zeng, L. Wang, L. Zeng, A. Shen, J. Hu, A label-free SERS probe for highly sensitive detection of Hg^{2+} based on functionalized Au @ Ag nanoparticles, *Talanta* 62 (2017) 374–379.
- [5] Z.Q. Tian, B. Ren, D.Y. Wu, Surface-enhanced Raman scattering: from noble to transition metals and from rough surfaces to ordered nanostructures, *J. Phys. Chem. B* 106 (2002) 9464–9483.
- [6] P. Podini, J.M. Schunr, Applicability of SERS to the study of adsorption at high pressure, *Chem. Phys. Lett.* 93 (1982) 86–90.
- [7] C.J. Sandroff, H.E. King Jr., D.R. Herschbach, High-pressure study of the liquid/solid interface: surface-enhanced Raman scattering from adsorbed molecules, *J. Phys. Chem.* 88 (1984) 5647–5653.
- [8] M. Bradley, J. Krech, Local environment of molecules adsorbed on colloids: a high-pressure- surface-enhanced Raman study, *J. Phys. Chem.* 99 (1995) 292–300.
- [9] K.E. Brown, D.D. Dlott, High-pressure Raman spectroscopy of molecular monolayers adsorbed on a metal surface, *J. Phys. Chem. C* 113 (2009) 5751–5757.
- [10] Y. Fu, E.A. Friedman, K.E. Brown, D.D. Dlott, Vibrational spectroscopy of nitroaromatic self-assembled monolayers under extreme conditions, *Chem. Phys. Lett.* 501 (2011) 369–374.
- [11] Y. Fu, J.M. Christensen, D.D. Dlott, Molecular adsorbates under high pressure: a study using surface-enhanced Raman scattering spectroscopy, *J. Phys. Conf. Ser.* 500 (2014).
- [12] Y. Fu, D.D. Dlott, Single molecules under high pressure, *J. Phys. Chem. C* 119 (2015) 6373–6381.
- [13] P. Wang, H. Li, C. Cui, J. Jiang, In-situ surface enhanced Raman spectroscopy detection in high pressure solution, *Appl. Surf. Sci.* 425 (2017) 833–837.
- [14] F. Tielsen, M. Saeys, J. Tourwe, An ab initio study of the interaction of SCN^- with a silver electrode: the prediction of vibrational frequencies, *J. Phys. Chem. A* 106 (2002) 1450–1457.
- [15] G. Hu, D. Han, G. Jia, T. Chen, Z. Feng, C. Li, Coadsorption of trimethyl phosphine and thiocyanate on colloidal silver: a SERS study combined with theoretical calculations, *J. Raman Spectrosc.* 40 (2009) 387–393.
- [16] X. Li, A.A. Gewirth, Potential-dependent reorientation of thiocyanate on Au electrodes, *J. Am. Chem. Soc.* 125 (2003) 11674–11683.
- [17] G. Cabello, X.J. Chen, R. Panneerselvam, Z.Q. Tian, Potential dependent thiocyanate adsorption on gold electrodes: a comparison study between SERS and SHINERS, *J. Raman Spectrosc.* 47 (2016) 1207–1212.
- [18] H. Wetzel, H. Gerischer, B. Pettinger, Surface-enhanced Raman scattering from silver-cyanide and silver-thiocyanate vibrations and the importance of adatoms, *Chem. Phys. Lett.* 80 (1981) 159–162.
- [19] M.J. Weaver, F. Barz, J.G. Dordon II, M.R. Philpott, Surface-enhanced Raman spectroscopy of electrochemically characterized interfaces; potential dependence of Raman spectra for thiocyanate at silver electrode, *Surf. Sci.* 125 (1983) 409–428.
- [20] P.P. Fang, J.F. Li, X.D. Lin, J.R. Anema, D.Y. Wu, B. Ren, Z.Q. Tian, A SERS study of

- thiocyanate adsorption on Au-core Pd-shell nanoparticle film electrodes, *J. Electroanal. Chem.* 665 (2012) 70–75.
- [21] Q. Yang, F. Liang, D. Wang, P. Ma, D. Gao, J. Han, Y. Li, A. Yu, D. Song, X. Wang, Simultaneous determination of thiocyanate ion and melamine in milk and milk powder using surface-enhanced Raman spectroscopy, *Anal. Methods-UK* 6 (2014) 8388–8395.
- [22] H. Luo, M.J. Weaver, Surface-enhanced Raman scattering as a versatile vibrational probe of transition-metal interfaces: thiocyanate coordination modes on platinum-group versus coinage-metal electrodes, *Langmuir* 15 (1999) 8743–8749.
- [23] P. Pienpinijtham, X. Han, S. Ekgasit, Y. Ozaki, Highly sensitive and selective determination of iodide and thiocyanate concentrations using surface-enhanced Raman scattering of starch-reduced gold nanoparticles, *Anal. Chem.* 83 (2011) 3655–3662.
- [24] L. Wu, Z. Wang, S. Zong, Y. Cui, Rapid and reproducible analysis of thiocyanate in real human serum and saliva using a droplet SERS-microfluidic chip, *Biosens. Bioelectron.* 62 (2014) 13–18.
- [25] X. Lin, W.L.J. Hasi, X.T. Lou, S. Lin, F. Yang, B.S. Jia, Y. Cui, D.X. Ba, D.Y. Lin, Z.W. Lu, Rapid and simple detection of sodium thiocyanate in milk using surface-enhanced Raman spectroscopy based on silver aggregates, *J. Raman Spectrosc.* 45 (2014) 162–167.
- [26] P.C. Lee, D. Meisel, Adsorption and surface-enhanced Raman of dyes on silver and gold sols, *J. Phys. Chem.* 86 (1982) 3391–3395.
- [27] M. Oćwieja, Z. Adamczyk, K. Kubiak, Tuning properties of silver particle monolayers via controlled adsorption-desorption processes, *J. Colloid. Interface Sci.* 376 (2012) 1–11.
- [28] G. Mie, *Annalen der physik*, 330, 1908, 377–445. doi: 10.1002/andp.19083300302.
- [29] A. Henglein, M. Giersig, Formation of colloidal silver nanoparticles: capping action of citrate, *J. Phys. Chem. B* 103 (1999) 9533–9539.
- [30] J. Widoniak, S. Eiden-Assmann, G. Maret, Silver particles tailoring of shapes and sizes, *Colloid. Surface A* 270–271 (2005) 340–344.
- [31] Y. Bao, B. Zhao, X. Tang, D. Hou, J. Cai, S. Tang, J. Liu, F. Wang, T. Cui, Tuning surface plasmon resonance by the plastic deformation of Au nanoparticles within a diamond anvil cell, *Appl. Phys. Lett.* 107 (2015) 201909.
- [32] C. Schmidt, M.A. Ziemann, In-situ Raman spectroscopy of quartz: a pressure sensor for hydrothermal diamond-anvil cell experiment at elevated temperatures, *Am. Mineral.* 85 (2000) 1725–1734.
- [33] R.A. Bailey, S.L. Kozak, T.W. Michelsen, W.N. Mills, Infrared spectra of complexes of the thiocyanate and related ions, *Coordin. Chem. Rev.* 6 (1971) 407–445.
- [34] P. Gans, J.B. Gil, D.P. Fearnley, Spectrochemistry of solutions. Part 14. Raman and infrared spectra of thiocyanatosilver (I) complexes in some non-aqueous solutions, *J. Chem. Soc. Dalton. Trans.* 8 (1981) 1708–1713.
- [35] D.S. Corrigan, J.K. Foley, P. Gao, S. Pons, M.J. Weaver, Comparison between surface-enhanced Raman and surface infrared spectroscopies for strongly perturbed adsorbated: thiocyanate at gold electrodes, *Langmuir* 1 (1985) 616–620.